ELSEVIER

Journal of Molecular Structure (Theochem) 501–502 (2000) 261–269

THEO CHEM

www.elsevier.nl/locate/theochem

Structural phase transitions in Na, Mg and Al crystals: dominant role of the valence in local pseudopotential theory ☆

J.P. Perdew[a], F. Nogueira[b,*], C. Fiolhais[b]

[a]*Department of Physics and Quantum Theory Group, Tulane University, New Orleans, LA 70118, USA*
[b]*Department of Physics, University of Coimbra, P3000 Coimbra, Portugal*

Abstract

Within a perturbative treatment of realistic local electron–ion pseudopotentials for the simple metals, we study structural phase transitions under pressure in Na and other monovalent metals, Mg and other divalent metals, and Al and other trivalent metals. For the "good local pseudopotential" metals Na, Mg, and Al, our results are in reasonable agreement with experiment. The sequence of predicted transitions between crystal structures, and the volume compression ratios V/V_0 at which these transitions are predicted, are determined largely by the valence z. The valence z also determines the dependence of the total energy upon the tetragonal c/a ratio along the Bain path from bcc to fcc. This path shows the divalent metals unstable in both fcc and bcc structures, and the trivalent metals unstable in bcc.

Keywords: Structural phase transitions; Local pseudopotential theory; Crystal structure

1. Introduction

As the properties of molecules and solids are determined by their valence electrons, it is convenient to neglect both the core electrons and the oscillations of the valence-electron orbitals in the cores. Then the interactions of the valence electrons among themselves may be described by density functional theory [1,2], and their effective interactions with the ionic cores by electron–ion pseudopotentials [3,4]. Cohen [5] has called this the "standard model" of electronic structure theory.

The simplest pseudopotentials are local or multiplicative operators [6–10], although greater realism can be achieved by using nonlocal [11–13] or angular-momentum-dependent potentials [14,15]. In the close-packed structures of the simple or sp-bonded metals, the pseudopotential may be regarded as a weak perturbation [3] on the electron gas of uniform density $\bar{n}$, the average valence electron density. The valence z (number of valence electrons per atom) is another important parameter.

We have recently constructed local pseudopotentials $w(r)$ for the interaction between an electron at r and a simple-metal ion centered at $r = 0$. These potentials (a) tend to $-z/r$ outside the core; (b) make the total energy of the close-packed crystal minimize at the observed equilibrium average valence electron density $\bar{n}_{\mathrm{eq}} = 3/(4\pi r_s^{\mathrm{eq}3})$; and (c) satisfy a third condition. For our "individual" pseudopotentials [16], this third condition is reproduction of the all-electron interstitial density at equilibrium. For our "universal" pseudopotentials [17], which depend upon $\bar{n}_{\mathrm{eq}}$ and z only, it is reproduction of the realistic

☆ Dedicated to Professor R. Gáspár on the occasion of his 80th year.

* Corresponding author.

0166-1280/00/$ - see front matter
PII: S0166-1280(99)00437-6

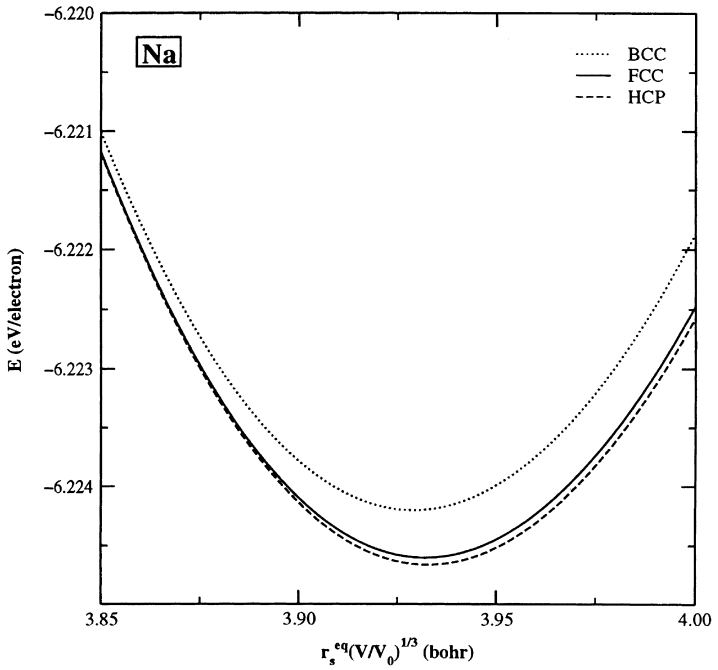

Fig. 1. Bulk binding energies per valence electron for Na in the bcc, fcc, and hcp structures, as functions of the average interelectron separation $r_s^{eq}(V/V_0)^{1/3}$. All the figures of this article show energies calculated to second order in the individual local pseudopotential of Ref. [16].

$\bar{n}_{eq}$-dependent bulk modulus from the stabilized jellium model with effective valence $z^* = 1$ [18]. We utilize the local density approximation [1,19,20] for the exchange-correlation energy, and second-order pseudopotential perturbation theory for the energy. Zero-point vibrational energy is neglected, as are finite-temperature effects. Details may be found in Refs. [16,17].

Our local pseudopotentials yield realistic bulk binding energies, bulk moduli and their derivatives, and shear moduli. For many of the simple metals, they also predict the observed zero-temperature equilibrium crystal structures and structural energy differences. Phonon frequencies [21,22], lattice instabilities [21,22], and liquid–metal resistivities [21] have also been calculated, and the transferability of our pseudopotentials to atomic or molecular environments has been studied [23].

In the present work, we investigate the predictions of our local pseudopotential for phase transitions of the simple metals under pressure at zero temperature among the face-centered cubic (fcc), body-centered cubic (bcc), and ideal hexagonal close-packed (hcp) structures. We also study energy along the continuous Bain path [24–27] which connects fcc to bcc at constant volume.

Qualitative aspects of our results are characteristic of the most-realistic local pseudopotentials, and controlled largely by the valence z. Because we get very similar figures from our individual and universal local pseudopotentials, only the former results will be reported here. (We use the individual pseudopotential as corrected in the erratum of Ref. [16].) We find very similar figures for all simple metals of a given valence: $z = 1$ (Li, Na, K, Rb, Cs), $z = 2$ (Be, Mg, Ca, Sr, Ba), and $z = 3$ (Al, Ga, In, Tl). Thus we shall report results only for that metal of each valence for which a local pseudopotential seems most appropriate: Na, Mg, and Al. These metals appear together in the same row of the periodic table, with p electrons in their cores and with all d-orbitals high above the Fermi energy. The dominant role that the valence z plays in the determination of crystal structure is consistent with the "universal phase diagrams" (structure maps in the $r_s^{eq} - z$ plane) we have presented elsewhere [17].

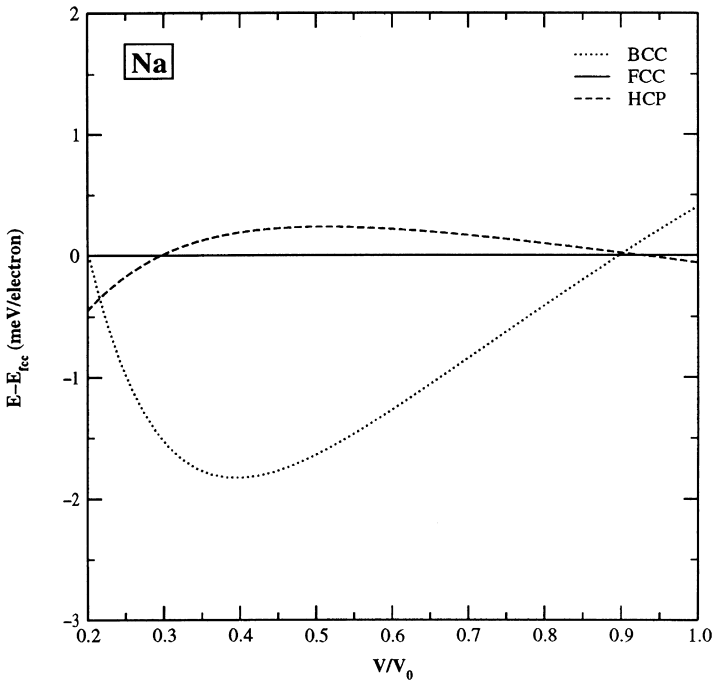

Fig. 2. Energy difference $E - E_{\mathrm{fcc}}$ per valence electron versus volume compression ratio V/V_0 for Na in three crystal structures. V_0 is the equilibrium volume per valence electron.

The energy differences between different close-packed crystal structures are small and delicate, as shown by Fig. 1 which plots the bulk binding energy per valence electron versus the average interelectron distance $r_s^{\mathrm{eq}}(V/V_0)^{1/3}$ for Na. In our formalism, they arise from the structure dependence of the Madelung and band-structure energies. We calculated the Madelung constants for all the structures (including the tetragonal ones) by the Ewald summation method; see Ref. [27, Fig. 2].

2. Structural phase transitions under pressure

For a given volume V per valence electron, the zero-temperature crystal structure minimizes the total energy E per valence electron. Figs. 2–4 display $E - E_{\mathrm{fcc}}$ vs. V/V_0, where V_0 is the equilibrium volume, for Na, Mg, and Al in the fcc, bcc, and hcp structures. Because the pseudopotential picture fails when the cores overlap, only the range $0.2 \leq V/V_0 \leq 1.0$ has been plotted.

For a given pressure $P = -\partial E/\partial V$, the zero-temperature crystal structure minimizes the total enthalpy $H = E + PV$ per valence electron. Since $\Delta H = 0$ at a transition, $\Delta E = -P\Delta V$ is the work needed to drive the transition. Figs. 5–7 display $H - H_{\mathrm{fcc}}$ vs. P.

According to Figs. 2 and 5, Na is hcp at zero pressure, but transforms under slight pressure first to fcc (at $P = 0.7 \times 10^{-2}$ Mbar) and then to bcc (at $P = 1.0 \times 10^{-2}$ Mbar); these pressures are too small to be seen on the scale of Fig. 5, and so are shown in an insert with an expanded scale. Na then remains bcc up to $P = 1.64$ Mbar, where it transforms back to hcp.

Because Na is well described by a weak local pseudopotential, these results are reasonably close to experiment. Na at zero temperature and pressure seems to have a 9R structure [28], with an enormous unit cell but otherwise similar to hcp [29]. There are signs of a transition to bcc at 0.1×10^{-2} or 0.2×10^{-2} Mbar [30]. Compression at room temperature does not show any change from bcc up to 0.27 Mbar [30]. Perturbative [31,32] and nonperturbative [33] calculations with nonlocal pseudopotentials place

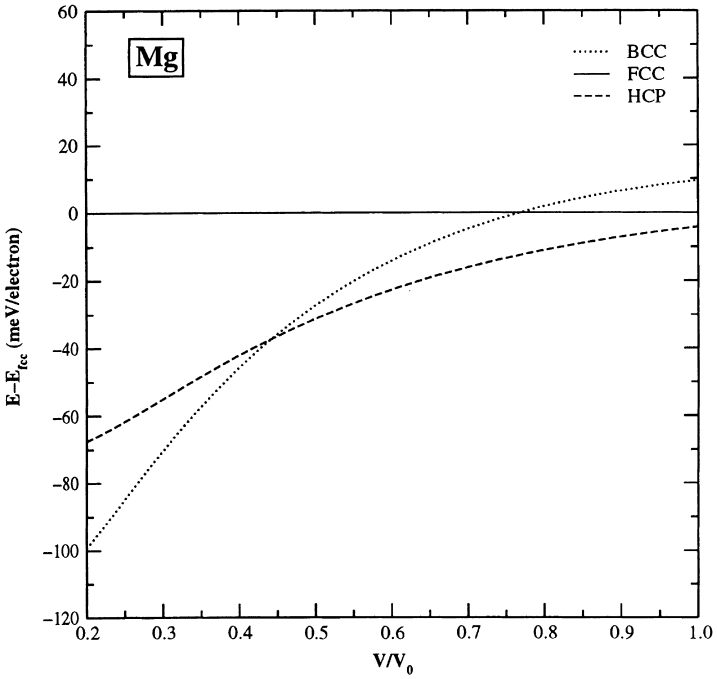

Fig. 3. Same as Fig. 2, but for Mg.

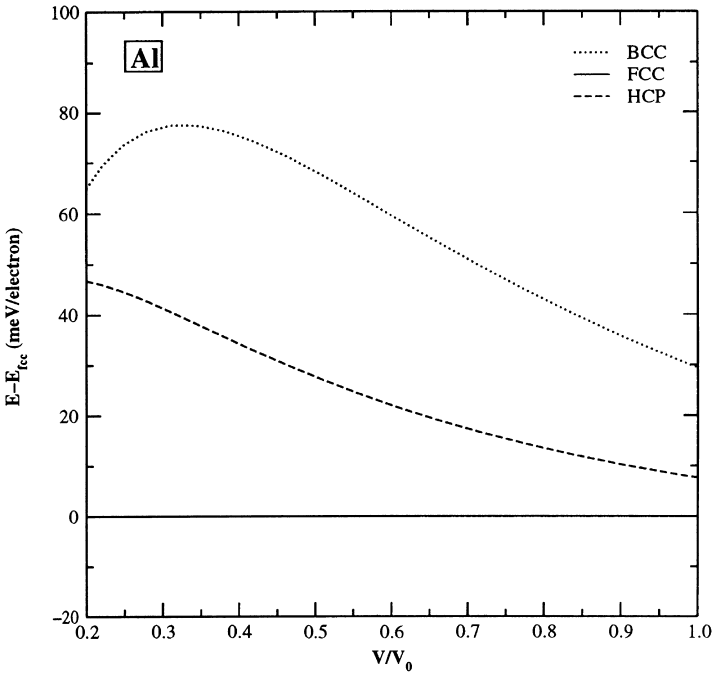

Fig. 4. Same as Fig. 2, but for Al.

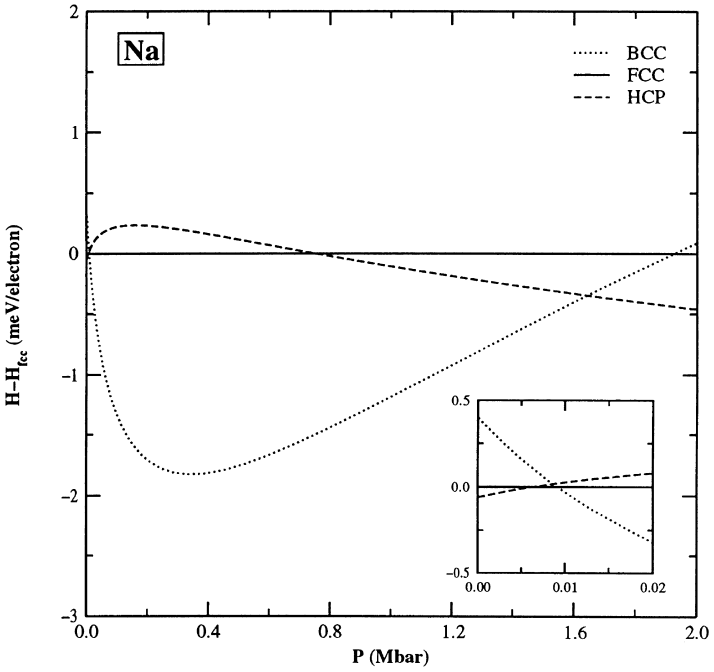

Fig. 5. Enthalpy difference $H - H_{fcc}$ per valence electron versus pressure P for Na in three crystal structures.

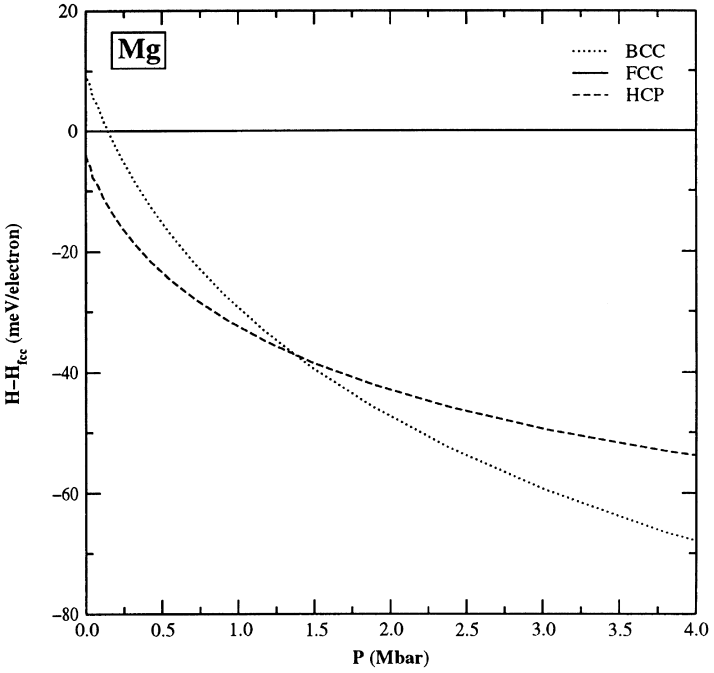

Fig. 6. Same as Fig. 5, but for Mg.

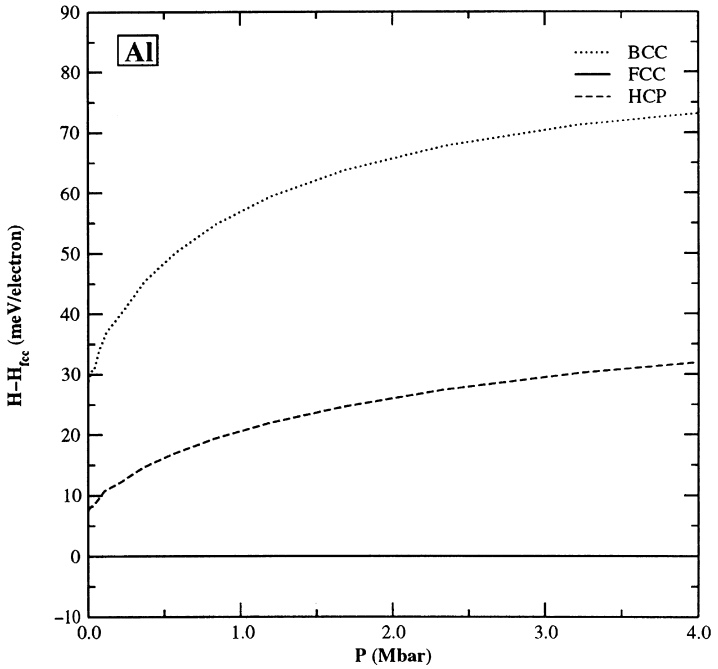

Fig. 7. Same as Fig. 5, but for Al.

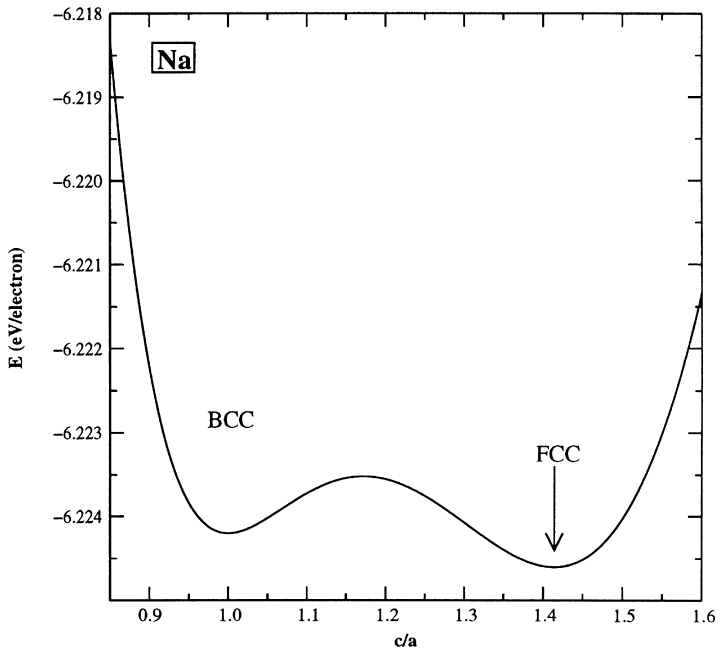

Fig. 8. Bulk binding energy E per valence electron versus c/a ratio for Na in the body-centered tetragonal phase along the Bain path.

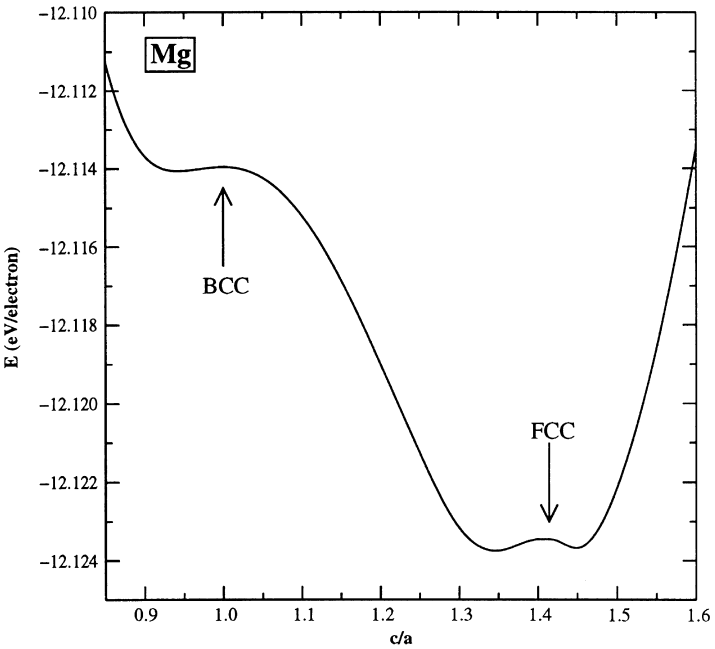

Fig. 9. Same as Fig. 8, but for Mg.

the zero-temperature hcp to bcc transition at 1.0×10^{-2} Mbar, without an fcc pocket of stability. The perturbative calculations [31] also show a transition from bcc to hcp at $P = 1.04$ Mbar.

In our local pseudopotential approximation, the other monovalent metals (Li, K, Rb, Cs) have figures very similar to Fig. 2 for Na. The principal difference is that the predicted crystal structure at $V/V_0 = 1$ is correctly bcc for K, Rb, and Cs, with the transition occurring for V slightly *greater* than V_0. The other divalent metals (Be, Ca, Sr, Ba) have curves similar to Fig. 3 for Mg, and the other trivalent metals (Ga, In, Tl) have curves similar to Fig. 4 for Al.

According to Figs. 3 and 6, Mg is hcp at zero pressure and transforms to bcc at $P = 1.37$ Mbar. Experiment [30] places this transition at $P = 0.50$ Mbar, closer to the predictions of perturbative [31,32,34] (0.50 Mbar) and nonperturbative [35] (0.60 Mbar) calculations with nonlocal pseudopotentials.

According to Figs. 4 and 7, Al remains fcc at all pressures. Experiment [36] has not shown any transition up to 2.19 Mbar, but a transition to hcp is predicted by perturbative [31,32] ($P = 3.60$ Mbar) and nonperturbative [37,38] ($P = 2.20$ Mbar) pseudopotential calculations, and a further transition to bcc is predicted at 5.60 Mbar [31,32] and 3.80 Mbar [37,38], respectively.

The bcc structure is more open (less closely packed) than the fcc or hcp structures. The transitions that occur under pressure from the less to the more open structure [30] have been explained as the result of increasing occupancy of nd orbitals under pressure [31,39]: the ns and np orbitals of a simple-metal atom lie much lower in energy than the nd orbitals, but are pushed up relative to the nd orbitals by the overlap that occurs under pressure. Interestingly, our perturbative treatment of a local pseudopotential is able to capture the transition to bcc, accurately for $z = 1$ but progressively less accurately for $z = 2$ and 3.

In fact, the limit $V/V_0 \rightarrow 0$ is one in which the Madelung energy dominates the band-structure energy in any local pseudopotential model, and so the limiting crystal structure of the static lattice is bcc, which minimizes the electrostatic energy of point ions on a lattice neutralized by a uniform negative background. However, because the Madelung constant for bcc is only slightly stronger than those for fcc or hcp, this limit is sometimes only achieved at very small V/V_0.

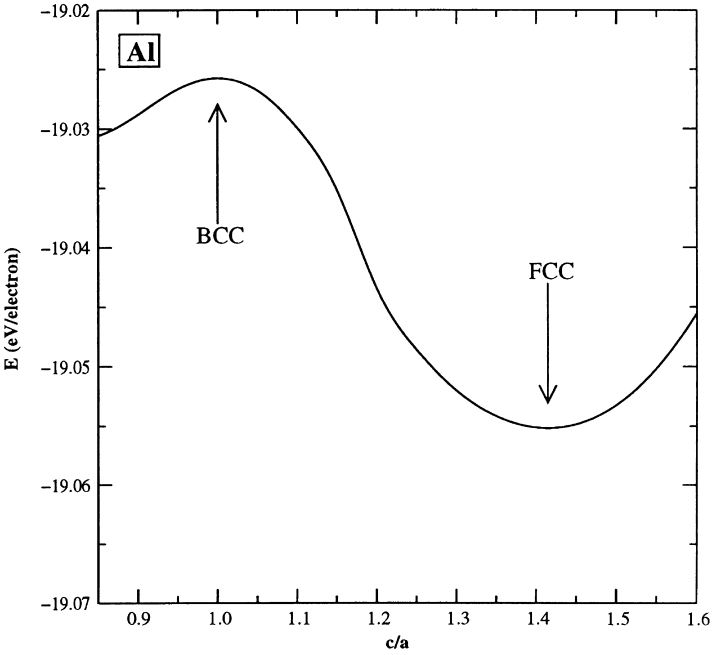

Fig. 10. Same as Fig. 8, but for Al.

3. Bain path from bcc to fcc

The body-centered tetragonal (bct) crystal structure has a c/a ratio which may be varied continuously at constant volume. For $c/a = 1$, bct reduces to bcc; for $c/a = \sqrt{2}$, bct reduces to fcc [24–27]. Figs. 8–10 show the total bulk binding energy per valence electron as a function of c/a for Na, Mg, and Al.

For Na and the other $z = 1$ metals, these are two energy minima, at the bcc and fcc values of c/a. This suggests that these structures are metastable or stable, with fcc more stable for Li and Na; and bcc more stable for K, Rb, and Cs.

For Mg and the other $z = 2$ metals, there is a weak energy maximum at the fcc value of c/a, surrounded by two shallow nearby minima, and an energy maximum or saddle point at the bcc value. In these metals, our local pseudopotential predicts that fcc and bcc are unstable against spontaneous lattice distortion.

For Al and the other $z = 3$ metals, there is an energy minimum at the fcc value of c/a, indicating the stability or metastability of that structure, and an energy maximum at the bcc value of c/a, indicating the instability of that structure.

The instabilities found here along the Bain path are confirmed by phonon soft-mode studies [21,22] with the same local pseudopotentials. The actual existence of divalent metals (Ca, Sr, Ba) in the bcc and fcc structures demonstrates that the local pseudopotential model is unsuitable for these alkaline earth metals, in which the unoccupied valence d orbitals lie close in energy to the occupied valence s and p orbitals of the atom.

4. Conclusion

Local pseudopotentials constructed for the bulk equilibrium volume of a simple metal may not transfer well to highly compressed volumes. For the phase transitions under pressure, local pseudopotentials seem fully satisfactory only for Na.

The local pseudopotential approximation is known to be more realistic for some simple metals (e.g. Na, Mg, Al) than for others. Within this approximation, the equilibrium crystal structures, the patterns of structural phase transitions under compression, and the various lattice instabilities of the simple metals are controlled largely by the valence z alone.

We have not shown results for the tetravalent

metals Sn and Pb, which in local pseudopotential theory are predicted to remain hcp for $0.2 \leq V/V_0 \leq 1.0$. For these metals, bcc has an unstable energy maximum (surrounded by neighboring minima) and fcc has a metastable energy minimum along the Bain path at $V/V_0 = 1.0$. While in Pb the fcc structure has the lowest energy along the Bain path, in Sn one of the minima near bcc has the lowest energy. Pb is in reality fcc, while Sn has a distorted diamond structure.

The simple metals display striking trends which have been observed but not fully explained in Ref. [17] and here: (1) Electronic properties are fixed largely by the equilibrium average valence electron density $\bar{n}^{eq}$ and valence z, with the bulk modulus controlled largely by $\bar{n}^{eq}$ alone. (2) Within the local pseudopotential approximation, crystal structure is controlled largely by z alone. Other trends in the simple metals are discussed in Ref. [17]. There are also many trends among the larger group of simple and transition metals which have been treated by Rose and coworkers [40–42].

Acknowledgements

This work was supported in part by the US National Science Foundation under Grant No. DMR98-10620, and in part by the Portuguese PRAXIS XXI program (Grant No. PRAXIS/2/2.1/FIS/473/94).

References

[1] W. Kohn, L.J. Sham, Phys. Rev. 140 (1965) A113.
[2] R.G. Parr, W. Yang, Density Functional Theory of Atoms and Molecules, Oxford University Press, New York, 1989.
[3] W.A. Harrison, Pseudopotentials in the Theory of Metals, Benjamin, New York, 1966.
[4] J. Hafner, From Hamiltonians to Phase Diagrams, Springer, Berlin, 1987.
[5] M.L. Cohen, Solid State Commun. 92 (1994) 45.
[6] H. Hellmann, Acta Physicochim. USSR 1 (1935) 913.
[7] H. Hellmann, Acta Physicochim. USSR 4 (1936) 225.
[8] H. Hellmann, Acta Physicochim. USSR 4 (1936) 324.
[9] H. Hellmann, J. Chem. Phys. 3 (1935) 61.
[10] R. Gáspár, I. Tamássy-Lentei, Acta Phys. Acad. Sci. Hung. 50 (1981) 343.
[11] J.C. Phillips, L. Kleinman, Phys. Rev. 116 (1959) 287.
[12] J.C. Phillips, L. Kleinman, Phys. Rev. 118 (1960) 1153.
[13] A. Nagy, I. Andrejkovics, Phys. Rev. A 53 (1996) 3656.
[14] D.R. Hamann, M. Schlüter, C. Chiang, Phys. Rev. Lett. 43 (1979) 1494.
[15] R. Gáspár, J. Szabo, J. Mol. Struct. (Theochem) 227 (1991) 87.
[16] C. Fiolhais, J.P. Perdew, S.Q. Armster, J.M. MacLaren, M. Brajczewska, Phys. Rev. B 51 (1995) 14 001 53 (1996) 13 193 (erratum).
[17] F. Nogueira, C. Fiolhais, J.P. Perdew, Phys. Rev. B 59 (1999) 2570.
[18] J.P. Perdew, H.Q. Tran, E.D. Smith, Phys. Rev. B 42 (1990) 11 627.
[19] R. Gáspár, Acta Physica (Hungary) 3 (1954) 263.
[20] J.P. Perdew, Y. Wang, Phys. Rev. B 45 (1992) 13 244.
[21] L. Pollack, J.P. Perdew, J. He, F. Nogueira, C. Fiolhais, Phys. Rev. B 55 (1997) 15 544.
[22] L. Pollack, J.P. Perdew, Int. J. Quantum Chem. 69 (1998) 359.
[23] F. Nogueira, C. Fiolhais, J. He, J.P. Perdew, A. Rubio, J. Phys.: Condens. Matter 8 (1996) 287.
[24] E.C. Bain, Trans. Am. Inst. Min. Metall. Engng 70 (1924) 25.
[25] T. Kraft, P.M. Marcus, M. Methfessel, M. Scheffler, Phys. Rev. B 48 (1993) 5886.
[26] P. Alippi, P.M. Marcus, M. Scheffler, Phys. Rev. Lett. 78 (1997) 3892.
[27] V.L. Sliwko, P. Mohn, K. Schwarz, P. Blaha, J. Phys.: Condens. Matter 8 (1996) 799.
[28] R. Berliner, H.G. Smith, J.R.D. Copley, J. Trivisonno, Phys. Rev. B 46 (1992) 14 436.
[29] C.S. Barrett, Acta Crystallogr. 9 (1956) 671.
[30] D.A. Young, Phase Diagrams of the Elements, University of California Press, Berkeley, CA, 1991.
[31] A.K. McMahan, J.A. Moriarty, Phys. Rev. B 27 (1983) 3235.
[32] J.A. Moriarity, A.K. McMahan, Phys. Rev. Lett. 48 (1982) 809.
[33] M.M. Dacorogna, M.L. Cohen, Phys. Rev. B 34 (1986) 4996.
[34] J.D. Althoff, P.B. Allen, R.M. Wentzcovitch, J.A. Moriarty, Phys. Rev. B 48 (1993) 13 253.
[35] R.M. Wentzcovitch, M.L. Cohen, Phys. Rev. B 37 (1988) 5571.
[36] R.G. Greene, H. Luo, A.L. Ruoff, Phys. Rev. Lett. 73 (1994) 2075.
[37] P.K. Lam, M.L. Cohen, Phys. Rev. B 24 (1981) 4224.
[38] P.K. Lam, M.L. Cohen, Phys. Rev. B 27 (1983) 5986.
[39] D.G. Pettifor, Bonding and Structure of Molecules and Solids, Clarendon Press, Oxford, 1995.
[40] J.H. Rose, H.B. Shore, Phys. Rev. B 43 (1991) 11 605.
[41] J.H. Rose, H.B. Shore, Phys. Rev. B 49 (1994) 11 588.
[42] M.M. Sigalas, J.H. Rose, D.A. Papaconstantopoulos, H.B. Shore, Phys. Rev. B 58 (1998) 13 438.